

Application of clotrimazole via a novel controlled release device provides potent retinal protection

著者	Zhaleh Kashkouli Nezhad
学位授与機関	Tohoku University
学位授与番号	11301甲第17466号
URL	http://hdl.handle.net/10097/00122350

博士論文

*Application of clotrimazole via a novel controlled release device provides
potent retinal protection*

(新規徐放デバイスを用いたクロトリマゾール投与による網膜保護効果)

東北大学大学院医学系研究科医科学専攻

細胞治療学分野

Zhaleh Kashkouli Nezhad

Summary

Introduction: Age-related macular degeneration (AMD) is a leading cause of blindness among older individuals. For chronic eye diseases such as AMD, optimum drug delivery system (DDS) to prolong the drug's effects, as well as discovering new therapeutic agents, is critical. In the case of posterior segment eye diseases, topical eye drop may be less effective due to the barrier function of corneal epithelium and tear fluid turnover. Therefore, intravitreal injection, which may be invasive to the eye, is clinically used and successful for AMD treatment. To release drug for several months and reduce the invasive procedure in the eye, my colleague have developed a transscleral drug delivery device as a reservoir type using photocurable resins. I investigated controlled release of clotrimazole (CLT), which was selected through screening of drug libraries as a potential candidate for retinal neuroprotection. I investigated whether clotrimazole (CLT) is capable of protecting retinal cells against oxidative-induced injury and the possible inhibitory effect of a sustained CLT-release device against light-induced retinal damage in rats.

Material and Methods: Mixtures of tri(ethylene glycol) dimethacrylate (TEGDM) and poly(ethylene glycol) dimethacrylate (PEGDM) can be easily molded into different substrate shapes by UV curing. Using these resins, a device that consists of a separately fabricated reservoir, a CLT formulation, and a controlled release cover have been fabricated. I investigated the in vitro release of CLT from the devices using HPLC. In vitro cell culture under oxygen/glucose deprivation (OGD), reactive oxygen species (ROS) detecting assay, western blotting were performed. The CLT-loaded devices were placed on the rat sclera and exposed to light to induce retinal damage and electroretinogram was conducted.

Results and Discussion: The in vitro results showed the release of CLT was successfully controlled by changing the PEGDM/TEGDM ratio in the cover. They also indicated pretreatment of immortalized retinal pigment epithelium cells (RPE-J cells) with 10-50 μM CLT before exposure to OGD conditions for 48 h decreased the extent of cell death, attenuated the percentage of ROS-positive cells, and decreased the levels of cleaved caspase-3. In vivo results showed that use of a CLT-loaded device lessened the reduction of electroretinographic amplitudes after light exposure.

Conclusion: We developed reservoir type DDS, which can continuously release a model drug for several weeks. This study shows for the first time the application of CLT as a potential drug against AMD. Additionally, prolonged sustained drug release using our device would be suitable for the treatment of chronic retinal diseases without disturbing intraocular tissues. Thus the administration of our clotrimazole-loaded device is expected to provide new tools for the treatment of retinal disorders.

Abbreviations	4
1. Abstract	5
2. Introduction	6
3. Methods	10
3.1 Materials	10
3.2 In vitro cell culture	10
3.3 Measurement of intracellular ROS levels	11
3.4 Western blot analysis	11
3.5 Device fabrication	12
3.6 In vitro release study	13
3.7 Implantation	14
3.8 Light exposure	14
3.9 Electroretinogram (ERG)	15
3.10 Statistical analysis	15
4. Results	17
4.1 In vitro protective effects of CLT against oxidation-induced cell death	17
4.2 Device fabrication and in vitro release study	18
4.3 In vivo protective effects of CLT against light-induced retinal damage in rats	18
5. Discussion	20
6. Conclusion	26
7. References	27
8. Figures and figure captions	34
Acknowledgments	42

Abbreviations

CLT	Clotrimazole
RPE-J	Retinal pigment epithelium cell line
OGD	Oxygen/glucose deprivation
ROS	Reactive oxygen species
TEGDM	Tri(ethylene glycol) dimethacrylate
PEGDM	Poly(ethylene glycol) dimethacrylate
AMD	Age-related macular degeneration
RPE	Retinal pigment epithelium
PBS	Phosphate-buffered saline
DMSO	Dimethyl sulfoxide
DMEM	Dulbecco's modified Eagle's medium
FBS	Fetal bovine serum
HPLC	High-performance liquid chromatography
MTS	3-(4,5-dimethylthiazol-2-yl)-5-(3-carboxymethoxyphenyl)- 2-(4-sulphophenyl)-2H-tetrazolium solution
ERG	Electroretinogram

1. Abstract

Retinal diseases, such as age-related macular degeneration (AMD) are leading cause of legal blindness among industrialized countries. Therefore, the development of new therapeutic agents and optimum drug delivery systems for its treatment are crucial. In this study, we investigate whether clotrimazole (CLT) is capable of protecting retinal cells against oxidative- induced injury and the possible inhibitory effect of a sustained CLT-release device against light-induced retinal damage in rats. In vitro results indicated pretreatment of immortalized retinal pigment epithelium cells (RPE-J cells) with 10–50 μ M CLT before exposure to oxygen/glucose deprivation conditions for 48 h decreased the extent of cell death, attenuated the percentage of reactive oxygen species-positive cells, and decreased the levels of cleaved caspase-3. The device consists of a separately fabricated reservoir, a CLT formulation, and a controlled release cover, which are made of poly(ethylene glycol) dimethacrylate (PEGDM) and tri(ethylene glycol) dimethacrylate (TEGDM). The release rate of CLT was successfully tuned by changing the ratio of PEGDM/TEGDM in the cover. In vivo results showed that use of a CLT-loaded device lessened the reduction of electroretinographic amplitudes after light exposure. These findings indicate that the application of a polymeric CLT loaded device may be a promising method for the treatment of some retinal disorders.

2. Introduction

Retinal diseases are main cause of blindness in the industrialized countries. These retinal diseases include age-related macular degeneration (AMD), retinitis pigmentosa, diabetic retinopathy and so on. AMD occurs primarily in elderly people and is the leading cause of legal blindness among older individuals in the developed world [1–3]. It has been predicted that as the population ages, there will be a 50% increase in the incidence of AMD before 2020 [4]. AMD is classified into two types: “dry” (atrophic or nonexudative) and “wet” (neovascular or exudative) forms. The “dry” form is the most common form (90%) and usually progresses slowly. The “wet” form is rare (10%), more severe, and may progress rapidly and cause the most severe vision loss. The characteristic lesions of dry AMD are soft drusen (63 micron or larger) and changes in pigmentation (hypo-, and/or hyperpigmentation) of the retinal pigment epithelium (RPE) [5]. In the early stages of AMD, which is asymptomatic, insoluble extracellular aggregates called drusen accumulate in the retina [6]. The late stage of dry AMD, which is also known as geographic atrophy (GA), is characterized by scattered or confluent areas of degeneration of retinal pigment epithelium (RPE) cells and the overlying light-sensing retinal photoreceptors, which rely on the RPE for trophic support [7]. In the wet type of AMD, new blood vessels grow and leak blood and fluid under the macula. This can lead to retinal detachment, scarring, and irreversible vision loss. Blood vessels grow in from the choriocapillaris under the retina (choroidal neovascularization; CNV). The vessels grow through Bruch’s membrane and spread under or above the RPE or both. These new blood vessels are very fragile, and easily leak and bleed. The consequences of abnormal vessel growth are hemorrhage and scar formation. This can damage the photoreceptors, and cause further vision loss [5]. The features of a healthy

ocular fundus, a representative eye with drusen, and a representative eye with CNV are shown in Fig. 1. Interestingly, pathologic features common to both types, including drusen and pigmentary changes in retinal pigment epithelial (RPE) cells, are limited in RPE cells and adjacent structures. Accordingly, pathophysiologically, AMD derives from pathologic alterations of retinal pigment epithelium (RPE) cells as well as its related tissues and their interactions with the local environment. RPE cells are basically prone to oxidative stress, high oxygen tension, lifelong light illumination, and phagocytosis [8]. Therefore, in accordance with the decrease of antioxidative enzymes in RPE cells with age, oxidative stress is thought to play a critical role in the pathogenesis of AMD [9]. In particular, reactive oxygen species (ROS) generation by oxidative stress induced by ischemia and hypoxia in the related area is considered to be a key factor in AMD pathophysiology [10]. High and sustained levels of ROS cause mitochondrial DNA damage and ultimately lead to the apoptosis of RPE cells [11]. Consequently, the RPE is one of the major ocular tissues affected by oxidative stress and is known to play an important role in pathogenesis of AMD [12]. Therefore, the protection of RPE cells against oxidative damage may be important in retinal protection for the treatment of AMD [13].

The development of optimum drug delivery systems is of great importance as well as the discovery of new therapeutic agents [14]. At present, one of the delivery methods is topical application. However, potential treatments for posterior segment diseases using this approach are hampered by the barrier function of corneal epithelium and tear fluid turnover [15]. Additionally, the molecular size and physical characteristics of the substance affect its topical delivery [16]. Soluble substrates pass easily through the sclera because of its high degree of hydration and low cell population [17]. We reported that low-molecular compounds could reach the RPE via a transscleral route, accumulate

around the RPE, and pass through the RPE into the neural retina [18]. Therefore, transscleral delivery is potentially a more applicable method for drug delivery to the posterior segment of the eye compared to topical application [19]. In chronic eye diseases such as AMD and retinitis pigmentosa, duration of effect with controlled drug release is critical. In this work, I used a previously reported polymeric device for transscleral delivery to the posterior segment of the eye [18]. The device comprises a microfabricated reservoir, controlled-release cover and drug formulations, which were made of photopolymerized tri(ethylene glycol) dimethacrylate (TEGDM) and poly(ethylene glycol) dimethacrylate (PEGDM) (Fig. 2). The device materials, PEGDM and TEGDM, are bio-inert and can be easily molded into different substrate shapes by UV curing [20, 21]. Thus, the device would appear to be stable and biocompatible for at least 1 year, and can be used to safely administer drugs by the transscleral approach without disturbing intraocular tissues. Once the device is fixed on the sclera, it would not need any additional treatments. Several months after implantation, stable scar covers outside of the device, enabling the device fixation. The surgical procedures including subconjunctival incision, device insertion, device fixation on the sclera, do not cause any intraocular invasion. Therefore, the device would be safer especially in intraocular tissue than traditional intraocular administrations such as intravitreal injections and intraocular implant. Furthermore in other experiments using rabbits, there was no toxic issue in the eye (retinal function by ERG, retinal tissue by OCT, intraocular tissue pressure) after device replacement (removal and re-implantation). So the implantation of the device on the sclera is almost no invasive in the eye.

Drug repositioning (drug reprofiling, drug repurposing) is gaining importance as the development of new drugs becomes increasingly expensive [22]. Although only a few compounds have been approved for new indications in the field of retinal

disorders, there are a number of substances with the potential to become reprofiled for new indications [23]. Clotrimazole, 1-[(2-Chlorophenyl)(diphenyl)methyl]-1H-imidazole (CLT), is a potent antimycotic drug, acting via the inhibition of sterol-14-demethylase, a cytochrome P-450-dependent enzyme [24]. CLT is currently used in human and veterinary medicine for the treatment of fungal infections [25]. It has been suggested that it could also be effective for the treatment of malaria and tuberculosis [26, 27]. Furthermore, the neuroprotective effects of CLT have been proven previously [28]. Studies have also demonstrated the effects of this drug on ovarian ischemia/reperfusion injury and liver ischemia/reperfusion injury [29, 30].

The objectives of the present study were to investigate whether CLT could protect RPE cells against oxidation-induced injury and to examine the sustained release of CLT using a previously described polymeric device [18] with a goal of repositioning CLT as a drug for retinal disease treatment. Excessive light exposure leads to photoreceptor degeneration in many animals [31, 32] and can be a risk factor for the onset and/or progression of AMD [33]. In these pathological conditions, ROS generation is involved in cell death [34, 35]. Thus, preliminary implantation of the CLT-loaded device on the sclera of rats was performed to evaluate its retinal protective effect against light-induced retinal injury.

3. Methods

3.1 Materials

CLT, dimethyl sulfoxide (DMSO), phosphate buffer saline (PBS) and penicillin (100 U/ml)/streptomycin (100 mg/ml) solution were purchased from Wako (Japan). Dulbecco's modified Eagle's medium (DMEM), fetal bovine serum (FBS) and L-glutamine were purchased from Gibco (Japan). A RPE cell line derived from primary cultures of RPE cells taken from 7-day-old Long-Evans rats (RPE-J cells) was purchased from ATCC (USA). Poly(ethylene glycol) dimethacrylate (PEGDM, Mn 750), tri(ethylene glycol) dimethacrylate (TEGDM, Mw 286.3) and 2-hydroxy-2-methylpropiophenone were purchased from Aldrich (USA). The reagents for high-performance liquid chromatography (HPLC) were purchased from Kanto Kagaku (Japan). Cell culture plates were purchased from BM equipment (Japan). A ProteoJET Cell Lysis kit was purchased from CosmoBio (Japan). SDS-PAGE reagents and electrophoresis gels were purchased from Biorad (Japan).

3.2 In vitro cell culture

RPE-J cells were maintained in DMEM (45 mM glucose) containing 4 % FBS, 1 % penicillin/streptomycin solution and 4 mM L-glutamine at 33 °C in a 5% CO₂ humidified incubator. The cells were plated in 96-well culture plates at a density of 2×10^4 cells/cm² and incubated for 48 h. After culturing the cells in media (0.1 ml) containing CLT at predetermined concentrations (including 0.03 % DMSO as a solvent for CLT) for 24 h, the cells were exposed to hypoxic conditions (2 % oxygen) with no

glucose (oxygen/glucose deprivation; OGD). The OGD exposure time was set to 48 h. Cell viability was assessed using a CellTiter 96 Aqueous One Solution Cell Proliferation Assay (Promega). 3-(4,5-dimethylthiazol-2-yl)-5-(3-carboxymethoxyphenyl)-2-(4-sulphophenyl)-2H-tetrazolium (MTS) solution mixed with medium in a ratio of 1:10 was applied to cells for 60 min and the MTS absorbance was measured at 492 nm (Fluoroscan Ascent).

3.3 Measurement of intracellular ROS levels

To assess the effect of CLT treatment on ROS generation, RPE-J cells were cultured in OGD condition as described above. CLT concentrations were set at 2–50 μ M. After culturing cells in 6-well culture plates, CellROX Orange Reagent (Invitrogen) was added directly to the cells in whole medium at a 1:500 dilution. Cells were incubated at 33°C for 30 min, centrifuged once to remove medium and excess dye, and then resuspended in PBS. Cells were then analyzed with a Tali Image-Based Cytometer (Invitrogen) using the red fluorescent protein channel, collecting 9 fields per sample [36]. Untreated cells, which were also labeled with CellROX Orange Reagent, were used to determine baseline levels of oxidative activity and to set the fluorescent threshold for the Tali instrument. This threshold was set manually and confirmed visually. All cells with signals greater than the threshold value were counted by the Tali instrument as positive.

3.4 Western blot analysis

RPE-J cells were cultured in OGD conditions by the same method described above. After treating cells with the indicated concentrations of CLT and exposing them to OGD conditions for 48 h, cells were washed with PBS, centrifuged, and then lysed using a ProteoJET Cell Lysis kit. Protein concentrations were determined using a bicinchoninic acid protein assay kit (Wako). Electrophoresis was performed using 4–15 % Tris–glycine gels. Proteins were transferred to PVDF membranes using a semidry transferring system (Biorad). The membranes were blocked with 5 % ECL blocking agent (GE Healthcare), incubated with primary antibodies against cleaved-caspase-3 (1:1000; Cell Signaling) and subsequently with the secondary antibody, horseradish peroxidase-linked IgG (1:10,000; Cell Signaling). After stripping the membranes of the antibodies for 10 min using reagents from a Western Re-Probe kit (Jackson Biotech), the membrane was probed in a similar manner for β -tubulin (1:2000; Cell Signaling). Bands were visualized using an enhanced chemiluminescence system (ECL Plus, GE Healthcare). Band intensities were measured using Image J software.

3.5 Device fabrication

The devices were fabricated as reported previously [18]. Briefly, the devices consist of a reservoir that can be loaded with a sustained release formulation of CLT and then sealed with a controlled release cover (Fig. 2). PEGDM and TEGDM including 1 % 2-hydroxy-2-methylpropiophenone as a photoinitiator were used as device materials. The reservoir was prepared by pouring TEGDM prepolymer into a microfabricated polydimethylsiloxane mold followed by UV light (LC8, Hamamatsu Photonics) photopolymerization for 40 s at an intensity of 11.6 mW/cm² [18]. The size of the reservoir was 2 mm \times 2 mm wide \times 1 mm high (drug-releasing surface area; 1.5 mm \times

1.5 mm = 2.25 mm²) for the rat experiments and 4 mm × 4 mm × 1.5 mm (drug-releasing surface area; 3.5 mm × 3.5 mm = 12.25 mm²) for the CLT releasing *in vitro* assay. The amount of CLT released from the device for the rat experiments was small and was very difficult to detect by standard HPLC technique, so we decided to use a larger device for the *in vitro* release study. For the sustained release formulation, CLT was dissolved in a mixture of a PEGDM/TEGDM prepolymer mixture (40 %/60 %) having a CLT concentration of 250 mg/mL, and the mixture was poured into a reservoir and photopolymerized for 40 s. The loading volume was 1.2 μL and 12 μL for the rat experiments and *in vitro* release study, respectively. After loading the drugs, the reservoirs were covered by applying a prepolymer mixture with the required ratios of PEGDM and TEDGM to the reservoirs followed by UV exposure for 4 min. The volume of the PEGDM/TEGDM prepolymer mixture was 1 and 5 μL for the rat experiments and *in vitro* release study, respectively. PEGDM/TEGDM prepolymer mixture ratios of 0 %/100 %, 20 %/80 %, 40 %/60 % and 60 %/40 % were designated as P0, P20, P40, and P60, respectively. The placebo device was prepared using PBS as a drug formulation.

3.6 In vitro release study

To demonstrate the controlled release of CLT, CLT was pelletized with P40 and loaded in the reservoirs, followed by sealing with P0, P20, P40 and P60 covers. Non-covered devices were prepared as controls. The devices were each incubated in 1.5 ml of PBS at 37°C. 750 μl of PBS was collected at different intervals and mixed with 750 μl of acetonitrile and the amounts of CLT that had diffused out of the devices were measured using HPLC (Prominence, Shimadzu). A Shim-pack VP-ODS (Shimadzu) was used as a

reversed-phase analytical column for CLT. The mobile phase of acetonitrile/10 mM sodium-phosphate buffer (pH 2.6) (4: 6, v/v) was delivered isocratically at 1 mL/min. The chromatograms were monitored at 215 nm. The devices were incubated in fresh PBS solution throughout the release study to ensure that the concentration of CLT would be below 20 % of its saturation value at all times. The results were expressed as amounts determined using a standard curve.

3.7 Implantation

Male Sprague–Dawley rats (SLC) weighing 250–300 g were used in this study. All animals were handled in accordance with the Association for Research in Vision and Ophthalmology Statement for the Use of Animals in Ophthalmic and Vision Research after receiving approval from the Institutional Animal Care and Use Committee of the Tohoku University Environmental & Safety Committee (No. 2013Mda-218). The rats were anesthetized with ketamine hydrochloride (90 mg/kg) and xylazine hydrochloride (10 mg/kg). Their ocular surfaces were anesthetized with a topical instillation of 0.4 % oxybuprocaine hydrochloride. A paralimbal conjunctival incision was made 1 mm from the temporal limbus. The devices were placed onto the left eyes at the sclera. Three groups (each group was n = 3) were set to examine the effect of controlled CLT-release on retinal protection against light injury; first is for treatment with CLT-loaded devices and second is placebo devices (three per group) as control of drug effect, and third is non-light-exposed rats with nontreatment as control of light-induced injury effect.

3.8 Light exposure

Seven days after device implantation, the unanesthetized rats were exposed to 8000 lux of white fluorescent light (Toshiba) for 24 h in automatically air-conditioned cages (22° C) with a reflective interior (NK system). Before the light exposure, the rats were dark-adapted for 24 h and the pupils were dilated with 1 % cyclopentolate hydrochloride eye drops (Santen) thirty minutes before light exposure.

3.9 Electroretinogram (ERG)

Four days after light exposure, flash ERGs were recorded as reported previously [37]. Briefly, after light exposure the rats were kept in the dark for 4 days until the flash ERGs were recorded (Purec, Mayo). The animals were anesthetized thirty minutes before the recording and the pupils were dilated with 1 % tropicamide and 2.5 % phenylephrine (Santen). Flash ERGs were recorded from the eyes of dark-adapted rats by placing a golden-ring electrode in contact (2.0 mm base curve, Mayo) with the cornea. An identical reference electrode was placed in the mouth, and a ground electrode was inserted subcutaneously near the tail. Single white-flash stimuli ranging from -3.5 to 0.5 log cd*s/m² were used. All procedures were performed in dim red light, and the rats were kept warm using a heating pad (FHC-HPS RM25906, Muromachi Kikai) at 37 °C during the entire procedure. The amplitude of the a-wave was measured from the baseline to the maximum a-wave peak, and the b-wave was measured from the maximum a-wave peak to the maximum b-wave peak.

3.10 Statistical analysis

Experimental data are presented as means \pm standard deviations (SD). Statistical significance was calculated with Ekuseru-Toukei 2012 (Social Survey Research Information), using an unpaired t test for normally distributed isolated pairs, and the analysis of variance (ANOVA) with Tukey's test for multiple comparisons. Differences were considered significant if $P < 0.05$ (*) or $P < 0.01$ (**).

4. Results

4.1 In vitro protective effects of CLT against oxidation-induced cell death

To investigate whether CLT could protect RPE-J cells against oxidative stress, and to clarify the effective doses of CLT, cells were pretreated with CLT and cultured under OGD conditions. An MTS assay was performed to evaluate cellular viability. The data confirmed that CLT-pretreated RPE-J cells showed significantly better cell survival under OGD conditions compared to non-pretreated cells and the increase in this viability was CLT-dose-dependent, i.e. administration of 10 μ M showed the highest protection (Fig. 3). These data indicated that CLT might protect RPEJ cells from oxidation-induced cell death.

To evaluate the preventive effects of CLT against ROS generation in RPE-J cells, these cells were pretreated with predetermined concentrations of CLT and exposed to OGD conditions. Results are shown as the proportions of ROS positive cells against negative ones. The data indicated that intracellular ROS was increased in the OGD condition as up to 40 % comparing to the normoxia group, which was, however significantly reduced by administration of 10, 20 and 50 μ M CLT treatment consequently (Fig. 4). These data indicated that inhibition of ROS generation by CLT application might protect RPE-J cells from oxidation-induced apoptosis.

Whether the cytoprotective effect of CLT on RPE-J cells is related to caspase-3 activity was assessed. RPE-J cells cultured under OGD-induced oxidative stress conditions exhibited elevated cleaved caspase-3 protein levels. The increased protein level was inhibited by pre-treatment with CLT (Fig. 5).

4.2 Device fabrication and in vitro release study

The device consists of a separately fabricated reservoir, a CLT formulation, and a controlled release cover (Fig. 6a). The CLT/P40 mixture (250 mg/mL CLT) was loaded into the reservoirs and the reservoirs were covered by different formulations of PEGDM/TEGDM polymer (P60, P40, P20, and P0). A prominent initial increase following a constant release was observed in the non-covered device (Fig. 6b). The constant release after a burst-like release is related to the sustained release formulation made of PEGDM/TEGDM. In the covered devices, a minor increase was observed initially, after which the release rate was almost constant and was dependent on the PEGDM/TEGDM ratio of the cover (Fig. 6b). The release rates estimated from the gradient curves for P60-, P40-, P20- and P0-covered devices were 1.86, 0.53, 0.20, and 0.01 $\mu\text{g}/\text{day}$, respectively. These results demonstrate the ability to control the release rate from a device by changing the ratio of PEGDM/TEGDM.

4.3 In vivo protective effects of CLT against light-induced retinal damage in rats

To determine the influence of sustained CLT administration by our controlled release device against light-induced retinal damage in rats, ERG amplitudes of a- and b-waves were measured (Fig. 8). Representative ERG spectra in which a- and b-waves are indicated with arrows are shown in Fig. 8a. Light exposure was performed 7 days after implantation when the acute inflammatory phase caused by device implantation might disappear. In the absence of CLT treatment, the ERG amplitudes in the light-exposed rats decreased to approximately 50 % of those of non-exposed rats. The amplitudes of a- and b-waves recorded from rats treated with CLT-loaded devices with P40-covers were

higher than those that received a placebo device treatment and comparable to those of non-light-exposed rats (Fig. 8b, c), and a statistically significant difference was observed in the amplitudes of b-waves (Fig. 8c).

5. Discussion

As CLT is administered via a transscleral route, the RPE should be the first retinal tissue exposed to released CLT. Our previous study showed that transsclerally delivered compounds may accumulate around the RPE [18]. The cumulative oxidative damage to RPE cells resulting from ROS generation is reported to be one of the pathological conditions in AMD [12]. Therefore, I first investigated the pharmacological action of CLT against RPE cells. CLT is a member of a large and structurally diverse group of azole fungicides that act by inhibiting cytochrome P450-dependent sterol 14-demethylases and hence are capable of blocking sterol synthesis [38]. CLT has been shown to have diverse effects on cellular metabolism and signaling pathways, particularly Ca^{2+} -dependent processes [24, 39]. Moreover, CLT has a free radical scavenger effect, which has been observed in several cell types [28]. Although these findings indicate that CLT might have both anti-oxidative and inflammatory effects, the focus of this study was on the anti-oxidative effects of this drug. It is important to note that AMD is a highly complex disease that is affected by multiple factors, such as ageing, genetic predisposition, environmental elements, oxidative stress, and inflammatory effects [40-42]. While inflammation has also been found to have a role in pathogenesis and progression of AMD, AMD is not a classic inflammatory disease [40]. There are many studies which highlight the role of oxidative stress in the pathogenesis of AMD and therefore the anti-oxidative effects of CLT was evaluated in this study. Anti-inflammatory function of CLT may also affect the results by CLT, which needs to be studied in the future. It is possible that the reduction in caspase-3 activity and ROS generation by CLT is causally associated with the inhibition of oxidative stress-induced cell death. Many researchers have investigated the efficacy of antioxidants such as

ascorbate [43, 44], dimethylthiourea [45], thioredoxin [46], phenyl-N-tert-butyl nitro [47, 48], and retinal defensive agents including superoxide dismutase against light-induced retinal damage [49]. However, many factors play a part in oxidative stress and ROS generation [50]. The mechanisms described above may be only partially responsible for the protective effect of CLT via its inhibition of oxidation induced cell death. The other possible mechanisms and pathways have yet to be elucidated.

The establishment of safe and effective methods for administering drugs to the retina has been an obstacle to developing effective new therapies for ocular disorders. In recent years, various drug delivery systems have been developed to circumvent the side effects of conventional methods including intravitreal injections, and to improve the ocular bioavailability of eye drop-administered drugs [51]. This study demonstrated that CLT can be applied via a polymeric drug delivery system [18] and can be released in a controlled manner. The ability to control the drug release is based on the swelling of the PEGDM/TEGDM polymer [18] (Fig. 7). A polymer made of short chains of TEGDM is likely to be compact, allowing practically no penetration of drugs. In fact, as pure TEGDM (P0) is almost impermeable to CLT, it enables unidirectional release to the sclera through the cover with negligible amounts through the TEGDM reservoir. In the other hand, long chains of PEGDM result in a greater tendency to swell and an open polymer network, facilitating permeation of CLT through the PEGDM/TEGDM cover. The drug loading of the devices used in the in vitro study was 3 mg ($250 \text{ mg/mL} \times 12 \text{ } \mu\text{L}$). Therefore, even in the case of the P60-covered device with a release rate of $1.86 \text{ } \mu\text{g/day}$, a sustained release for over 4 years may be possible. Consequently, CLT could be released in a controlled release manner by a PEGDM/TEGDM system. Non-covered device also shows constant release after initial burst. So if the device was washed to remove the burst release, it may be useful for DDS. But the release period may be short

compared to covered-devices due to the wash. It is also important to note that it is not yet clear whether the burst release is harmful or not. The harmful dose of CLT by intravitreal and topical drop should be studied in the future, if we are going to apply our system for human. Therefore, it is not yet clear whether no-covered device requires wash process or not.

Electroretinographic evaluation is one of the most widely used methods to determine visual function in animal models [52-55]. It is a standard electrophysiological measure used to assess the in vivo function of visual pathways and allows for long-term and non-invasive recordings in both humans and animals. This measurement has the advantage of robust behavior and do not require the rat to be trained, allowing a rapid evaluation of visual features. Furthermore, the key strength of the ERG is the ability to isolate signals from different classes of retinal neurons by changing the light adaption status, stimulus conditions, and data processing parameters [56]. Waveform analysis is one of the means of distinguishing the activities of different retinal cell types by ERG recording. The first negative deflection, termed the “a-wave,” derives mainly from the primary retinal neurons, the photoreceptors, whereas the following positive peak, designated the “b-wave,” mainly reflects responses from the downstream bipolar neurons [57] (a and b-waves are indicated in Fig. 8a by arrows). Assess the visually evoked potentials (VEPs) is another electrophysiological measurement to assess the in vivo visual function but due to technical limitations, I could not perform this test. Therefore, for the in vivo study, the drug release device was applied to a light-induced retinal injury model and retinal function was evaluated using an electroretinogram (ERG). Preliminary implantation study in rats shows that a CLT-loaded device implanted on the sclera could protect retinal function against light injury, based on measurements of ERG amplitudes. In the rat experiments, the amounts released would

be less than the release profiles shown in Fig. 6b, because I used a smaller device for the in vivo study than used in the in vitro release assay. The larger device used in the in vitro study had 5.44 times larger drug-releasing surface area (12.25 mm² vs. 2.25 mm²) and 3.42 times faster release rate than that of the device used in rats [58]. Therefore, the actual release rate and the duration of release in the rat experiments might be from one-third to one-fifth of the in vitro release profiles shown in Fig. 6b. As the in vitro cell culture results showed a protective effect at 10 μM (0.34 μg/mL)-CLT administration, the P40-covered device for rats, which may have a release rate of between 0.10–0.17 μg/day (one-fifth to one-third of 0.53 μg/day) was used in the in vivo study. Significant attenuation of b-wave amplitude reductions by CLT administration might indicate a potent protection of photoreceptors. Generally a-wave is derived from photoreceptors (outer retina), and b-wave is derived from bipolar cells, amacrine cells, and ganglion cells (inner retina). The results may suggest that CLT was more effective on rescuing the inner retinal cell. However, the value of a-wave is basically smaller than b-wave; therefore it is possible that by increasing the sample size, a more significant difference would be observed.

In another study, my colleagues have also evaluated the safety of device implantation. That study showed that there was no difference in then ERG amplitudes from device-implanted eyes versus non-treated eyes 8 weeks after implantation suggesting that the device could be used to safely administer drugs by the transscleral approach without disturbing intraocular tissues [37] (Fig 8d). As other in vivo experiments, I evaluated the expression of TUNEL-positive cells and assessed the outer nuclear layer (ONL) thickness in rats treated with CLT-loaded device and rats treated with placebo-device. These experiments did not show any differences between the two groups of rats. I believe the reason behind these data was the size of the device, which

was not large enough to be able to hold higher amounts of CLT; therefore, made it difficult to get expected results from histological analysis. It is also possible that defect in detecting the differences was because of the short implantation time and it would be possible that a longer implantation time would make it possible to detect the expected differences. Furthermore, usually ERG is more sensitive than histology and this may affect the results obtained from these experiments.

A limitation of this study is the lack of data on the pharmacokinetics of CLT in the eye, because the rat eyeballs were too small to measure the level of CLT in the retina using HPLC. Although my colleague has analyzed the transport of fluorescents as model drugs into the eye from the device [18], the quantification of the CLT distribution in the eye requires using larger animals and needs special techniques, such as liquid chromatography/mass spectrometry/mass spectrometry (LC-MS/MS). Additionally, the duration of the effect and the appearance of side effects after long-term implantation remain to be determined. To further support the CLT-mediated retinal protection, I am planning on carrying out a classical histological analysis of retinal sections and protein/gene expression assays in the future using animals with larger eyes. I suggest that the neuro-protective effect of CLT was related to its prolonged release from the device. However, to clarify this suggestion, as controls, intravitreal injections and topical eye drops of CLT should be studied in the future. Light induced retinal injury model is a temporal injure model. So for studying the long-term effect of CLT-DDS, a chronic retinal degeneration model such as transgenic S334ter rats or transgenic rabbits harboring Pro347/Leu rhodopsin gene should be used.

Furthermore, there is a growing awareness of the limitations of animal research and its inability to make reliable predictions for human clinical trials [59]. The problem with most of today's animal studies is that they rarely predict exactly what will happen in the

clinic, because the doses, formulations and schedules of medication differ from those given to the animals [60]. Similarly the drug delivery system in this study also encounters with limited ability of animal models to mimic exactly the extremely complex process of human physiology and also the difference of the eye size between humans, which affects the effective doses of the applied drug and the size and the implantation method of the delivery device. Therefore, animal models are another complication in translating the results of the in vivo findings to human models. Regardless of all these limitations; this is the first study showing CLT as a promising candidate for the treatment of visual impairment caused by AMD. In addition, the pathophysiology of other retinal diseases such as diabetic retinopathy and glaucoma is similar to AMD. These retinal diseases may have some common pathological background, such as oxidative stress and ROS generation which have been indicated to play a part in these diseases [61]. Therefore, there is hope that the therapeutic demonstration on AMD could be considered as a viable option for the family of retinal diseases. The drug delivery device was designed to support a number of practical clinical and therapeutic characteristics such as suture fixation to the sclera; multiple drug formulations, and shape flexible manufacturing to meet the curvature of the eyeball. The release profiles can be adjusted to meet therapeutic needs through the amount of contributing materials composition to the manufactured device, as well as through adjusting physical parameters such as thickness. Additionally, prolonged sustained drug release by using this device would be suitable for the treatment of chronic retinal diseases without disturbing intraocular tissues. Thus the administration of our clotrimazole-loaded device is expected to provide new tools for the treatment of retinal disorders.

6. Conclusion

In summary, the present study reveals that CLT can protect RPE-J cells against OGD-induced oxidative stress via the suppression of ROS generation and caspase-3 activity. Furthermore, a sustained CLT release system was established and its potent retinal protective effects demonstrated using a light-induced retinal damage animal model. I conclude that CLT may be a promising candidate for the treatment of visual impairment caused by AMD.

7. References

1. Hageman GS, Luthert PJ, Victor Chong NH, Johnson LV, Anderson DH, Mullins RF. An integrated hypothesis that considers drusen as biomarkers of immune-mediated processes at the RPE-Bruch's membrane interface in aging and age-related macular degeneration. *Prog Retin Eye Res.* 2001; 20(6):705–32.
2. Klein R, Klein BE, Linton KL. Prevalence of age-related maculopathy. The Beaver Dam Eye Study. *Ophthalmology.* 1992; 99(6):933–43.
3. Vingerling JR, Dielemans I, Hofman A, Grobbee DE, Hijmering M, Kramer CF, de Jong PT. The prevalence of age-related maculopathy in the Rotterdam Study. *Ophthalmology.* 1995; 102(2):205–10.
4. Friedman DS, O'Colmain BJ, Munoz B, Tomany SC, McCarty C, de Jong PT, Nemesure B, Mitchell P, Kempen J. Prevalence of age-related macular degeneration in the United States. *Arch Ophthalmol.* 2004; 122(4):564–72.
5. Birch, D. G. and F. Q. Liang. Age-related macular degeneration: a target for nanotechnology derived medicines. *Int J Nanomedicine.* 2007; 2(1): 65-77.
6. Bird, A. C. Therapeutic targets in age-related macular disease. *J Clin Invest.* 2010; 120(9): 3033-41.
7. Ambati, J. and B. J. Fowler. Mechanisms of age-related macular degeneration. *Neuron.* 2012; 75(1): 26-39.
8. Roth F, Bindewald A, Holz FG. Key pathophysiologic pathways in age-related macular disease. *Graefes Arch Clin Exp Ophthalmol.* 2004; 242(8):710–6.
9. Samiec, P. S., C. Drews-Botsch, et al. Glutathione in human plasma: decline in association with aging, age-related macular degeneration, and diabetes. *Free Radic Biol Med.* 1998; 24(5): 699-704.

10. Winkler BS, Boulton ME, Gottsch JD, Sternberg P. Oxidative damage and age-related macular degeneration. *Mol Vis*. 1999; 5:32.
11. Cai, J., M. Wu, et al. Oxidant-induced apoptosis in cultured human retinal pigment epithelial cells. *Invest Ophthalmol Vis Sci*. 1999; 40(5): 959-66.
12. Beatty S, Koh H, Phil M, Henson D, Boulton M. The role of oxidative stress in the pathogenesis of age-related macular degeneration. *Surv Ophthalmol*. 2000; 45(2):115–34.
13. Sur A, Kesaraju S, Prentice H, Ayyanathan K, Baronas-Lowell D, Zhu D, Hinton DR, Blanks J, Weissbach H. Pharmacological protection of retinal pigmented epithelial cells by sulindac involves PPAR-alpha. *Proc Natl Acad Sci USA*. 2014; 111(47):16754–9.
14. Del Amo EM, Urtti A. Current and future ophthalmic drug delivery systems. A shift to the posterior segment. *Drug Discov Today*. 2008; 13(3–4):135–43.
15. Hughes PM, Olejnik O, Chang-Lin JE, Wilson CG. Topical and systemic drug delivery to the posterior segments. *Adv Drug Deliv Rev*. 2005; 57(14):2010–32.
16. Prausnitz MR, Noonan JS. Permeability of cornea, sclera, and conjunctiva: a literature analysis for drug delivery to the eye. *J Pharm Sci*. 1998; 87(12):1479–88.
17. Olsen TW, Edelhauser HF, Lim JI, Geroski DH. Human scleral permeability. Effects of age, cryotherapy, transscleral diode laser, and surgical thinning. *Invest Ophthalmol Vis Sci*. 1995; 36(9):1893–903
18. Nagai N, Kaji H, Onami H, Ishikawa Y, Nishizawa M, Osumi N, Nakazawa T, Abe T. A polymeric device for controlled transscleral multi-drug delivery to the posterior segment of the eye. *Acta Biomater*. 2014; 10(2):680–7.
19. Geroski DH, Edelhauser HF. Transscleral drug delivery for posterior segment disease. *Adv Drug Deliv Rev*. 2001; 52(1):37–48.

20. Benoit, D. S., A. R. Durney, et al. Manipulations in hydrogel degradation behavior enhance osteoblast function and mineralized tissue formation. *Tissue Eng.* 2006; 12(6): 1663-73.
21. Kalachandra, S. Influence of fillers on the water sorption of composites. *Dent Mater.* 1989; 5(4): 283-8.
22. Wang ZY, Zhang HY. Rational drug repositioning by medical genetics. *Nat Biotechnol.* 2013; 31(12):1080–2.
23. Fowler BJ, Gelfand BD, Kim Y, Kerur N, Tarallo V, Hirano Y, Amarnath S, Fowler DH, Radwan M, Young MT, Pittman K, Kubes P, Agarwal HK, Parang K, Hinton DR, Bastos-Carvalho A, Li S, Yasuma T, Mizutani T, Yasuma R, Wright C, Ambati J. Nucleoside reverse transcriptase inhibitors possess intrinsic anti-inflammatory activity. *Science.* 2014; 346(6212):1000–3.
24. Yoshida Y, Aoyama Y. Interaction of azole antifungal agents with cytochrome P-45014DM purified from *Saccharomyces cerevisiae* microsomes. *Biochem Pharmacol.* 1987; 36(2):229–35.
25. Vanden Bossche H, Marichal P, Gorrens J, Coene MC, Willemsens G, Bellens D, Roels I, Moereels H, Janssen PA. Biochemical approaches to selective antifungal activity. Focus on azole antifungals. *Mycoses.* 1989; 32(Suppl 1):35–52.
26. Tiffert T, Ginsburg H, Krugliak M, Elford BC, Lew VL. Potent antimalarial activity of clotrimazole in in vitro cultures of *Plasmodium falciparum*. *Proc Natl Acad Sci USA.* 2000; 97(1):331–6.
27. McLean KJ, Marshall KR, Richmond A, Hunter IS, Fowler K, Kieser T, Gurcha SS, Besra GS, Munro AW. Azole antifungals are potent inhibitors of cytochrome P450 mono-oxygenases and bacterial growth in mycobacteria and streptomycetes. *Microbiology.* 2002; 148(Pt 10):2937–49.

28. Isaev NK, Stelmashook EV, Dirnagl U, Andreeva NA, Manuhova L, Vorobjev VS, Sharonova IN, Skrebitsky VG, Victorov IV, Katchanov J, Weih M, Zorov DB. Neuroprotective effects of the antifungal drug clotrimazole. *Neuroscience*. 2002; 113(1):47–53.
29. Iannelli A, de Sousa G, Zucchini N, Peyre L, Gugenheim J, Rahmani R. Clotrimazole protects the liver against normothermic ischemia-reperfusion injury in rats. *Transplant Proc*. 2009; 41(10):4099–104.
30. Osmanagaoglu MA, Kesim M, Yulug E, Mentese A, Karahan SC. Ovarian-protective effects of clotrimazole on ovarian ischemia/ reperfusion injury in a rat ovarian-torsion model. *Gynecol Obstet Invest*. 2012; 4(2):125–30.
31. Hayami K, Unoki K. Photoreceptor protection against constant light-induced damage by isopropyl unoprostone, a prostaglandin F(2alpha) metabolite-related compound. *Ophthalmic Res*. 2001; 33(4):203–9.
32. Imai S, Inokuchi Y, Nakamura S, Tsuruma K, Shimazawa M, Hara H. Systemic administration of a free radical scavenger, edaravone, protects against light-induced photoreceptor degeneration in the mouse retina. *Eur J Pharmacol*. 2010; 642(1–3):77–85.
33. Cruickshanks KJ, Klein R, Klein BE. Sunlight and age-related macular degeneration. The Beaver Dam Eye Study. *Arch Ophthalmol*. 1993; 111(4):514–8.
34. Murphy MP. Modulating mitochondrial intracellular location as a redox signal. *Sci Signal*. 2012; 5(242):pe39.
35. Wang YX, Zheng YM. ROS-dependent signaling mechanisms for hypoxic Ca²⁺ responses in pulmonary artery myocytes. *Antioxid Redox Signal*. 2010; 2(5):611–23.
36. Remple K, Stone L. Assessment of GFP expression and viability using the tali image-based cytometer. *J Vis Exp*. 2011; doi:10. 3791/3659.

37. Nagai N, Kaji H, Onami H, Katsukura Y, Ishikawa Y, Nezhad ZK, Sampei K, Iwata S, Ito S, Nishizawa M, Nakazawa T, Osumi N, Mashima Y, Abe T. A platform for controlled dual-drug delivery to the retina: protective effects against light-induced retinal damage in rats. *Adv Healthc Mater.* 2014; 3(10):1555–60 1524.
38. Sheehan DJ, Hitchcock CA, Sibley CM. Current and emerging azole antifungal agents. *Clin Microbiol Rev.* 1999; 12(1):40–79.
39. Burdon RH, Rice-Evans C. Free radicals and the regulation of mammalian cell proliferation. *Free Radic Res Commun.* 1989; 6(6):345–58.
40. Coleman, H. R., C. C. Chan, et al. Age-related macular degeneration. *Lancet.* 2008; 372(9652): 1835-45.
41. Klein, R., B. E. Klein, et al. Fifteen-year cumulative incidence of age-related macular degeneration: the Beaver Dam Eye Study. *Ophthalmology.* 2007; 114(2): 253-62.
42. Klein, R., K. J. Cruickshanks, et al. The prevalence of age-related macular degeneration and associated risk factors. *Arch Ophthalmol.* 2010; 128(6): 750-8.
43. Li ZY, Tso MO, Wang HM, Organisciak DT. Amelioration of photic injury in rat retina by ascorbic acid: a histopathologic study. *Invest Ophthalmol Vis Sci.* 1985; 26(11):1589–98.
44. Organisciak DT, Wang HM, Li ZY, Tso MO. The protective effect of ascorbate in retinal light damage of rats. *Invest Ophthalmol Vis Sci.* 1985; 26(11):1580–8.
45. Organisciak DT, Darrow RM, Jiang YI, Marak GE, Blanks JC. Protection by dimethylthiourea against retinal light damage in rats. *Invest Ophthalmol Vis Sci.* 1992; 33(5):1599–609.
46. Tanito M, Masutani H, Nakamura H, Ohira A, Yodoi J. Cytoprotective effect of thioredoxin against retinal photic injury in mice. *Invest Ophthalmol Vis Sci.* 2002; 43(4):1162–7.

47. Ranchon I, Chen S, Alvarez K, Anderson RE. Systemic administration of phenyl-N-tert-butyl nitron protects the retina from light damage. *Invest Ophthalmol Vis Sci.* 2001; 42(6):1375–9.
48. Tomita H, Kotake Y, Anderson RE. Mechanism of protection from light-induced retinal degeneration by the synthetic antioxidant phenyl-N-tert-butyl nitron. *Invest Ophthalmol Vis Sci.* 2005; 46(2):427–34.
49. Dong A, Shen J, Krause M, Akiyama H, Hackett SF, Lai H, Campochiaro PA. Superoxide dismutase 1 protects retinal cells from oxidative damage. *J Cell Physiol.* 2006; 208(3):516–26.
50. Dong A, Shen J, Krause M, Hackett SF, Campochiaro PA. Increased expression of glial cell line-derived neurotrophic factor protects against oxidative damage-induced retinal degeneration. *J Neurochem.* 2007; 103(3):1041–52.
51. Agnihotri SM, Vavia PR. Diclofenac-loaded biopolymeric nanosuspensions for ophthalmic application. *Nanomedicine.* 2009; 5(1):90–5.
52. Cuenca, N., L. Fernandez-Sanchez, et al. Correlation between SD-OCT, immunocytochemistry and functional findings in an animal model of retinal degeneration. *Front Neuroanat.* 2014; 8: 151.
53. Machida, S., M. Kondo, et al. P23H rhodopsin transgenic rat: correlation of retinal function with histopathology. *Invest Ophthalmol Vis Sci.* 2000; 41(10): 3200-9.
54. Pinilla, I., R. D. Lund, et al. Enhanced cone dysfunction in rats homozygous for the P23H rhodopsin mutation. *Neurosci Lett.* 2005; 382(1-2): 16-21.
55. Cuenca, N., I. Pinilla, et al. Regressive and reactive changes in the connectivity patterns of rod and cone pathways of P23H transgenic rat retina. *Neuroscience.* 2004; 127(2): 301-17.

56. Tomiyama, Y., K. Fujita, et al. Measurement of electroretinograms and visually Evoked potentials in awake moving mice. *PLoS One*. 2016; 11(6): e0156927.
57. Weymouth, A. E. and A. J. Vingrys. Rodent electroretinography: methods for extraction and interpretation of rod and cone responses. *Prog Retin Eye Res*. 2008; 27(1): 1-44.
58. Onami H, Nagai N, Kaji H, Nishizawa M, Sato Y, Osumi N, Nakazawa T, Abe T 2013. Transscleral sustained vasohibin-1 delivery by a novel device suppressed experimentally-induced choroidal neovascularization. *PLoS One* 8(3):e58580.
59. Perel P, Roberts I, Sena E, Wheble P, Briscoe C, Sandercock P, Macleod M, Mignini LE, Jayaram P, Khan KS. Comparison of treatment effects between animal experiments and clinical trials: systematic review. *BMJ*. 2007; 334(7586):197.
60. Ledford H. Translational research: 4 ways to fix the clinical trial. *Nature*. 2011; 477(7366):526–8.
61. Nita, M., x, et al. The Role of the Reactive Oxygen Species and Oxidative Stress in the Pathomechanism of the Age-Related Ocular Diseases and Other Pathologies of the Anterior and Posterior Eye Segments in Adults. *Oxidative Medicine and Cellular Longevity* 2016; 23.

8. Figures and figure captions

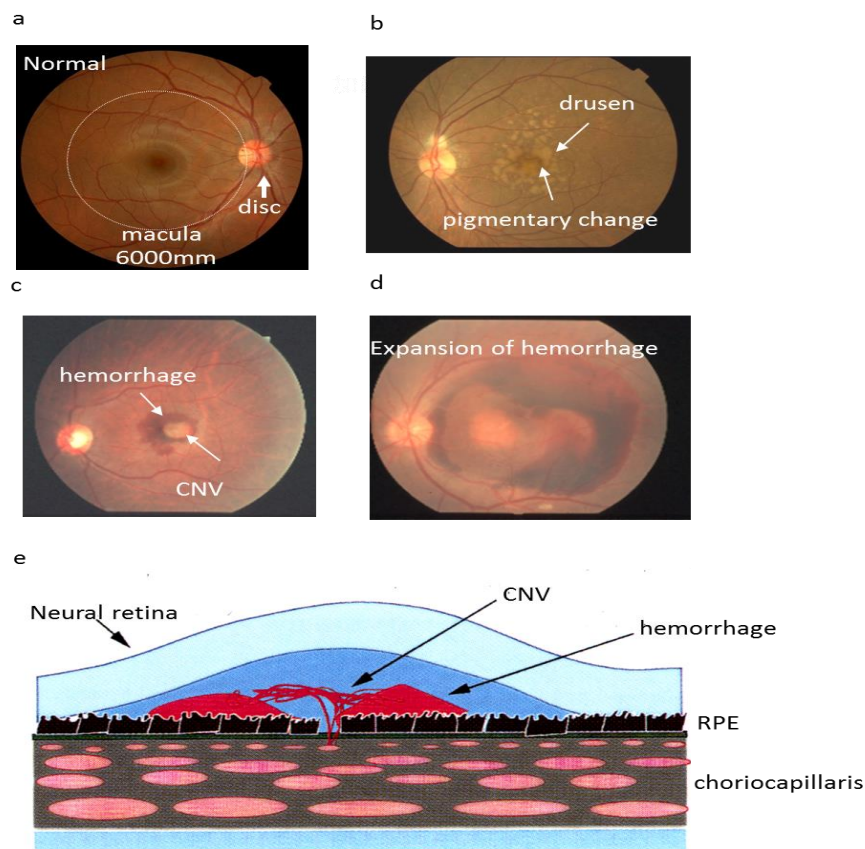


Fig. 1.

a The features of a healthy ocular fundus. Macular area is shown as 6000 diameter from fovea centralis. **b** A representative eye with early AMD. Picture shows drusen and pigmentary change of RPE. **c** A representative eye with CNV. CNV is generated in the macula and hemorrhage is obvious. **d** Shows expansion of the hemorrhage. **e** Shows how the blood vessels grow inward toward the choroid and transgress the RPE to grow in the subretinal space and cause hemorrhage.

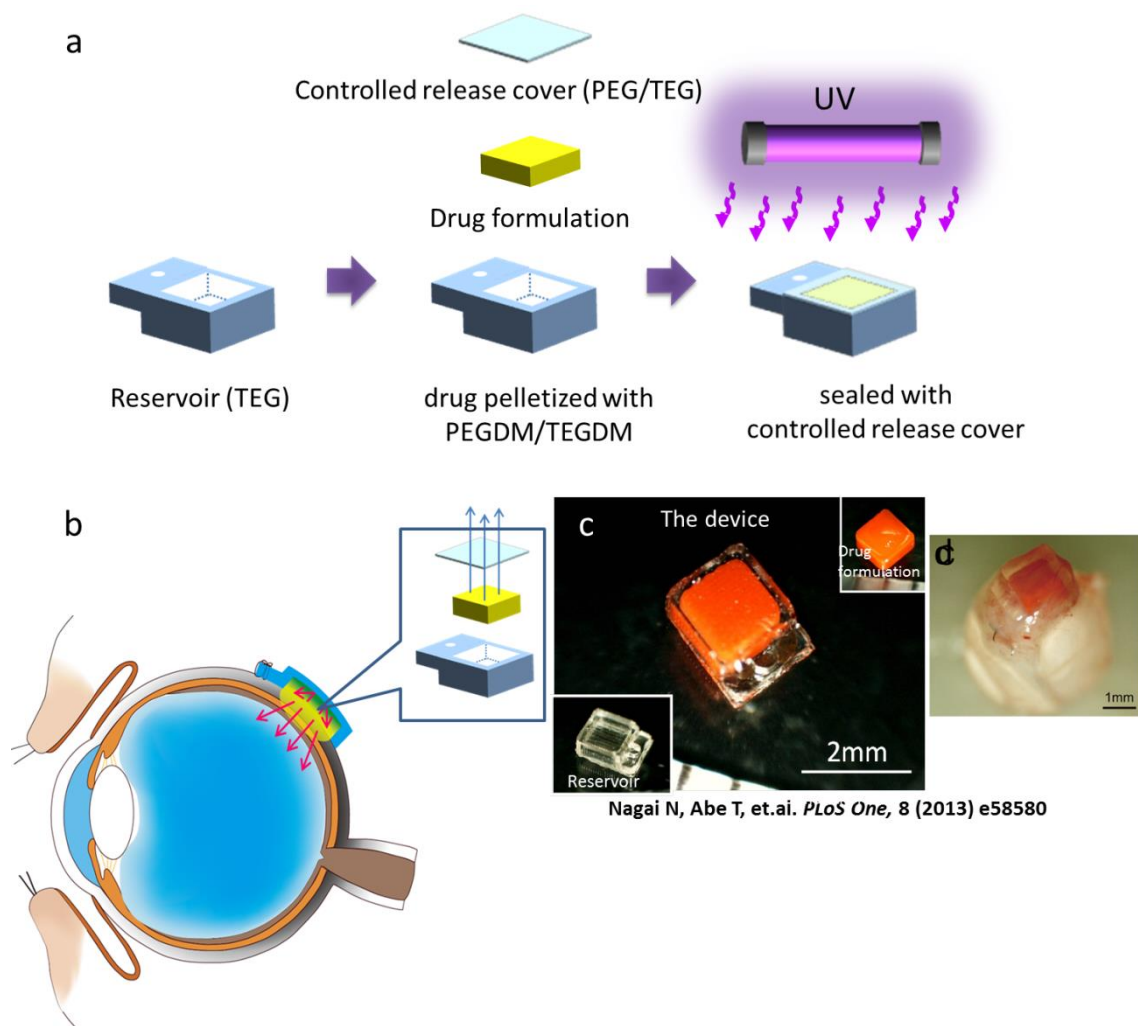


Fig. 2.

a Image shows assembling process of the device that consists of the drug formulation pelletized with PEGDM/TEGDM, a reservoir made of TEGDM and a controlled release cover made of PEGDM/TEGDM. After loading the pellets in the reservoir, the cover was sealed on the reservoir by UV curing. **b** Schematic image of transscleral intraocular multi-drug delivery using a polymeric device placed on the sclera. **c** photograph of the complete device containing fluorescein as a model drug. Scale bar, 2 mm. **d** Photograph of the rat eye where the device was implanted on the sclera. Scale bar, 1 mm.

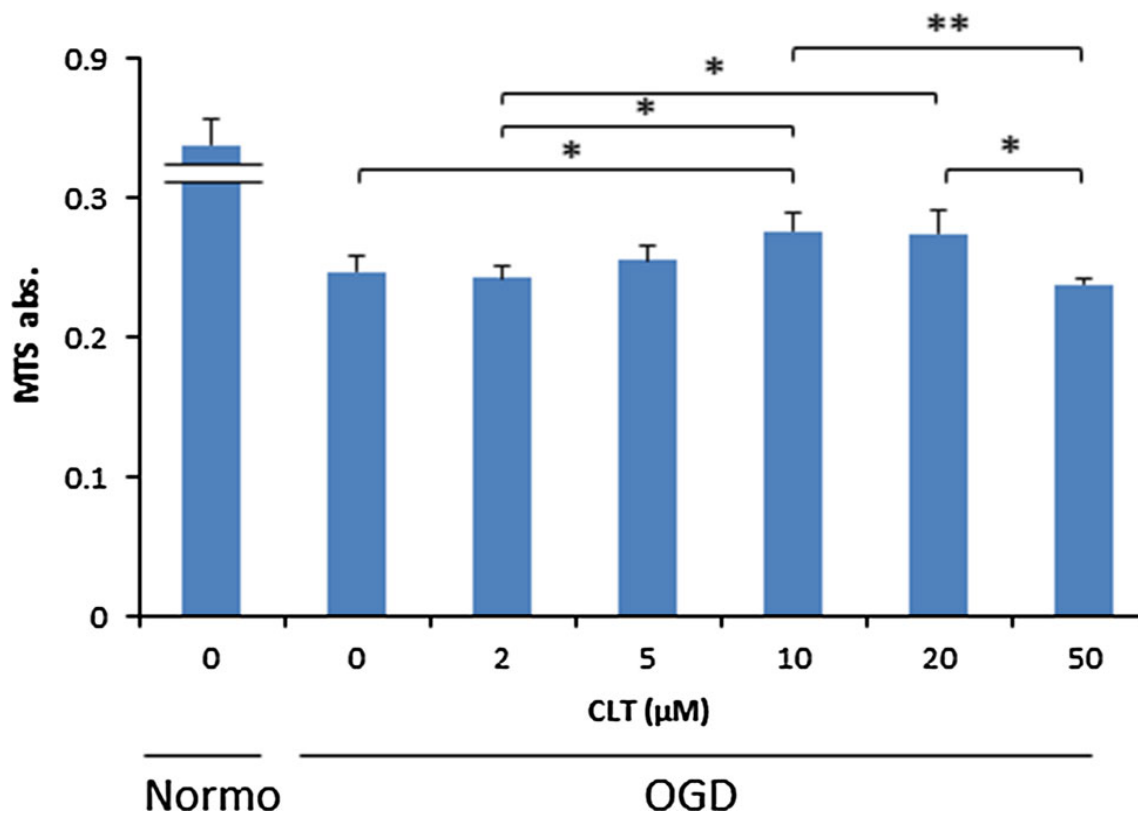


Fig. 3.

In vitro protective effects of administering different concentrations of CLT on the viability of RPE-J cell cultures under OGD stress conditions. Cell viability was measured using an MTS assay. Values are mean \pm SD; n = 7. *P < 0.05., **P < 0.01.

Abbreviations: Normo; normoxia.

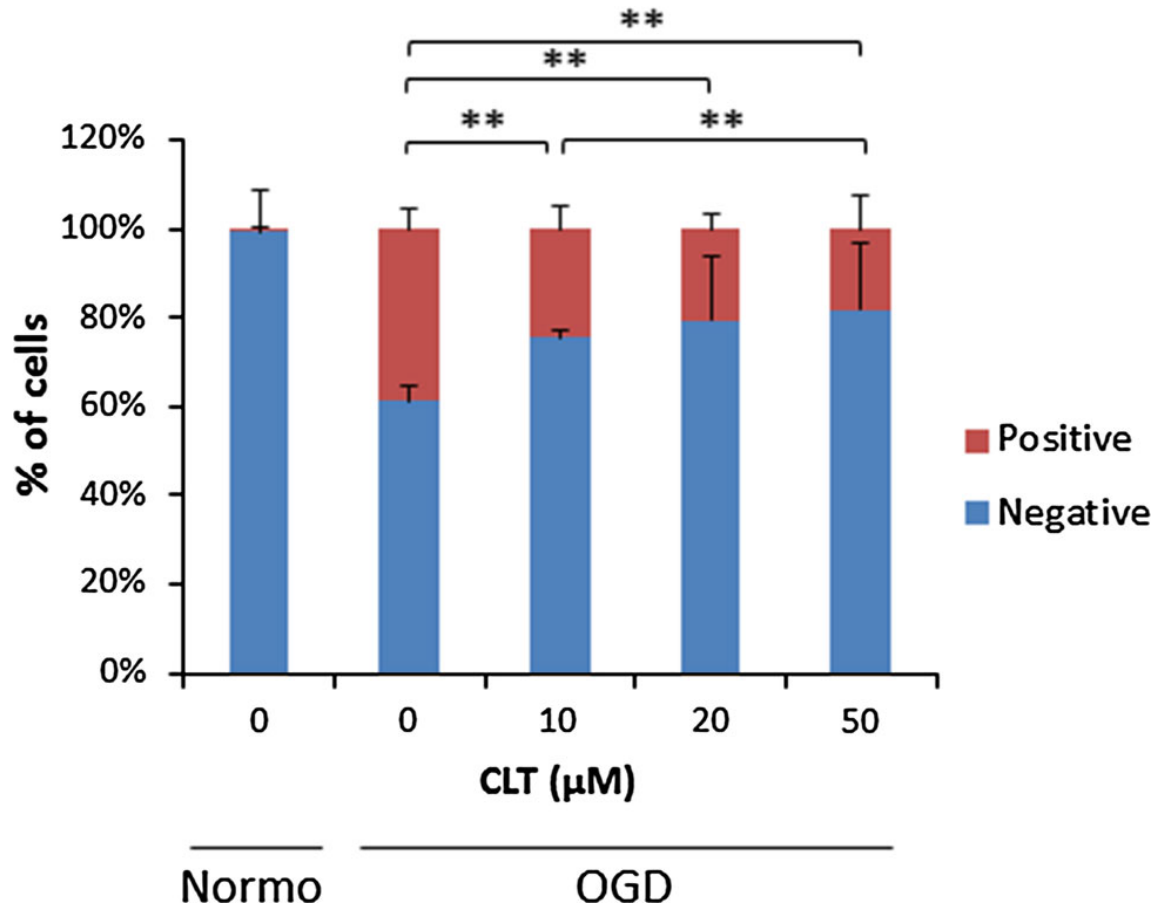


Fig. 4.

In vitro effects of CLT administration on ROS generation in RPE-J cell cultures under OGD stress conditions. ROS generation was assessed using a CellROX reagent and ROS-positive cells were measured by a Tali system (Invitrogen). Values are mean \pm SD; n = 7. *P < 0.05., **P < 0.01. Abbreviations: Normo; normoxia.

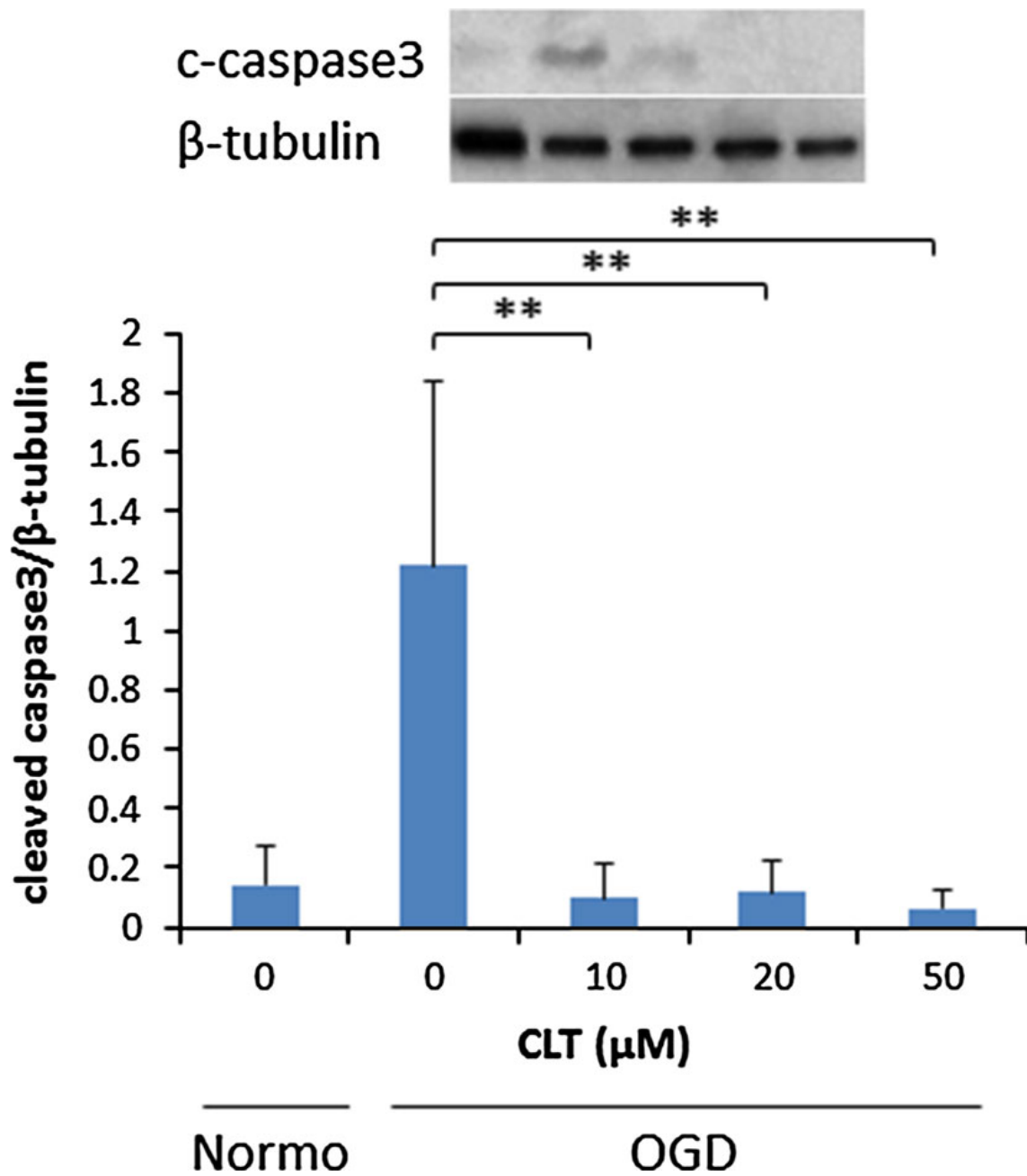


Fig. 5.

Western blotting of cleaved caspase-3 in CLT-pretreated RPE-J cells cultured under OGD conditions. The band intensities relative to beta-tubulin are shown in the bar graph.

Values are mean \pm SD; n = 7. *P < 0.05., **P < 0.01. Abbreviations: Normo; normoxia.

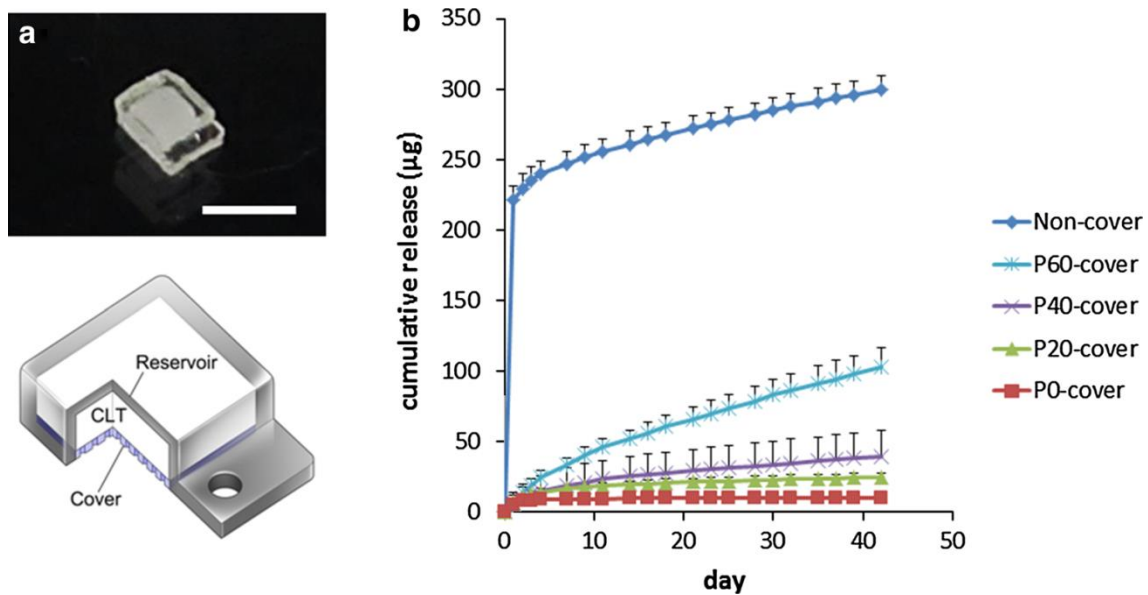


Fig. 6.

Transscleral intraocular drug delivery system and in vitro release of CLT from drug delivery devices. **a** Image shows a device that consists of the CLT pelletized with PEGDM/TEGDM, a reservoir made of TEGDM, and a controlled release cover made of a PEGDM/TEGDM mixture. **b** Release profiles of the drug delivery device consisting of CLT pelletized with P40 and various types of cover (P0, P20, P40, and P60) or non-cover. Values are mean \pm SD; n = 4

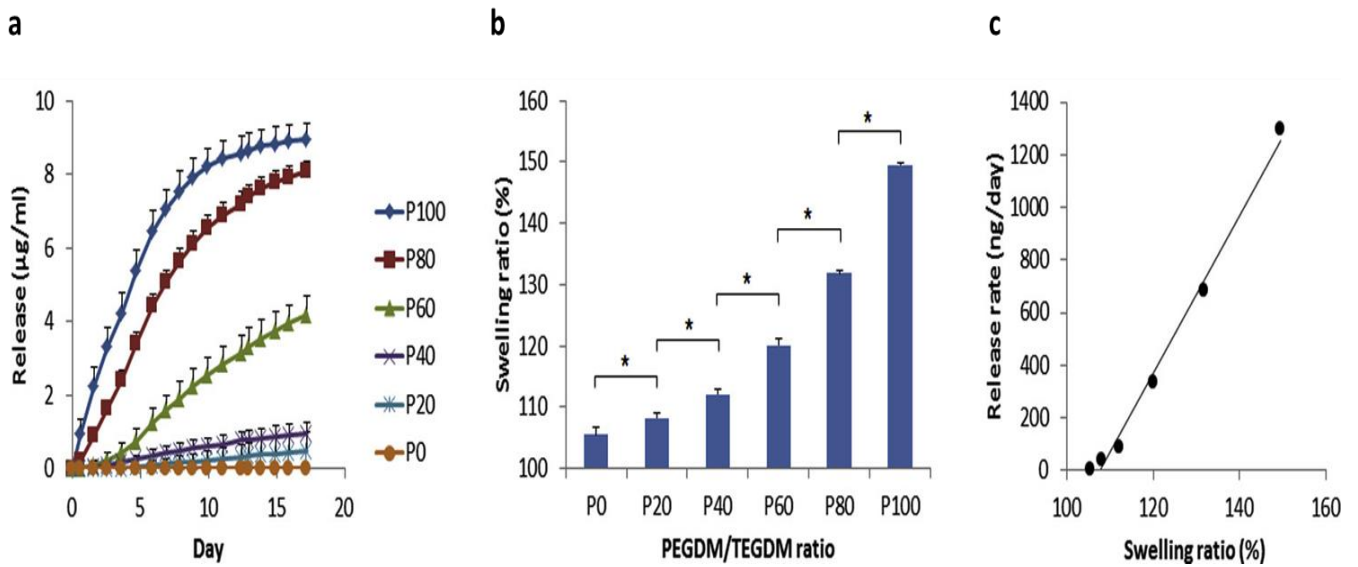


Fig. 7.

a Permeability of FL in PBS through the PEGDM/TEGDM reservoir with various PEGDM/TEGDM ratios. The release was assessed by monitoring the increase in fluorescence in the external PBS solution with time. **b** Swelling ability in PBS of PEGDM/TEGDM polymers (size: 5 mm × 5mm × 2 mm) with various PEGDM/TEGDM ratios. **c** Correlation between swelling ratio in **b** and release rate. Release rate was estimated from the slope of the curve of the line at the initial stable release period in **a**. Values are mean ± SD. * $p < 0.05$ (one-way analysis of variance (ANOVA) with Tukey's test).

N. Nagai et al. / Acta Biomaterialia 10 (2014) 680–687

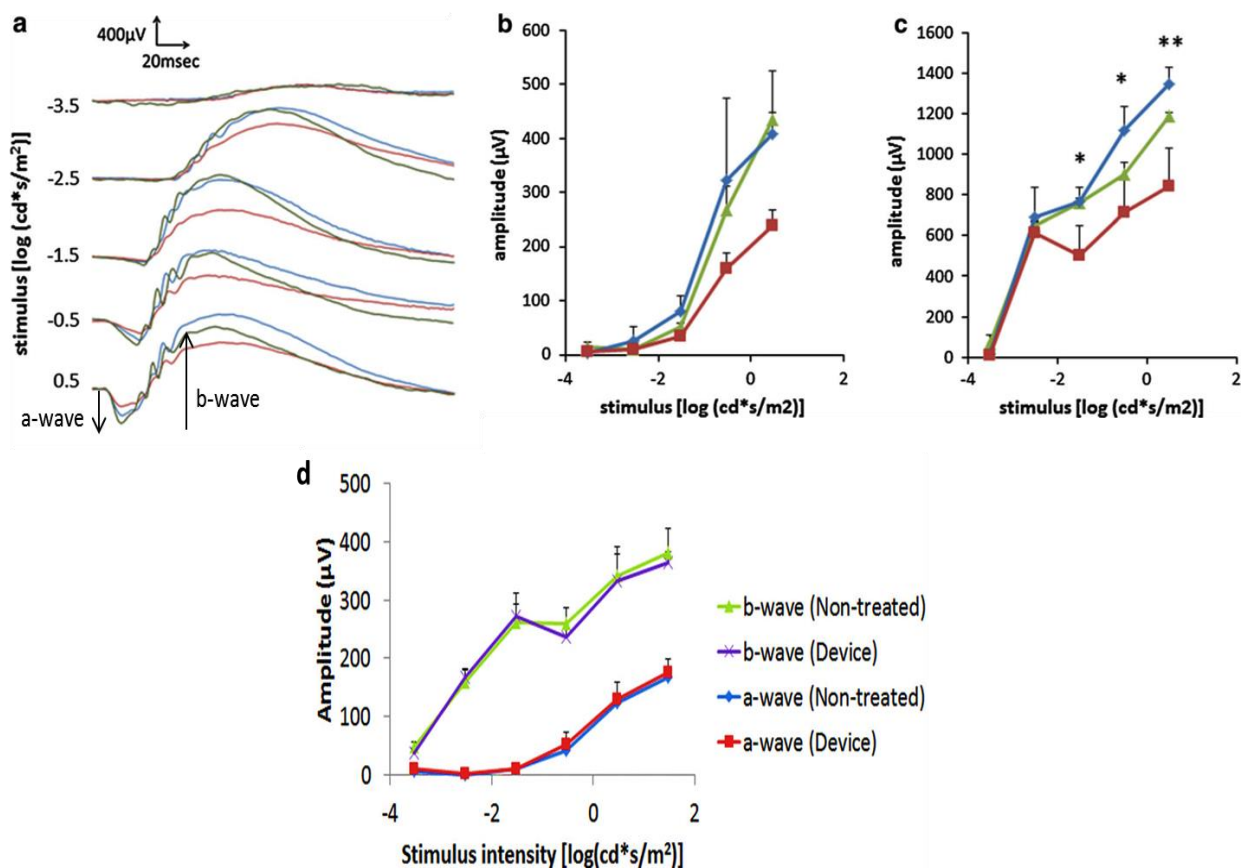


Fig. 8.

Effect of sustained CLT administration using this device on retinal protection. **a** Representative ERG spectra (*blue diamonds* CLT-loaded device-treated rats, *red squares* Placebo treated rats, *green triangles* non-light-exposed rats with non-treatment) and ERG amplitudes of **b** a- and **c** b-waves in the P40-covered device-treated group. Values are mean \pm SD; n = 3. *P < 0.05, **P < 0.01. **d** ERG amplitudes 8 weeks after implantation. Scale bar: 10 mm. Values are mean \pm SD.

8d. Nagai et al. *Adv. Healthcare Mater.* **2014**, 3, 1555–1560

Acknowledgments

First and foremost I would like to express my special appreciation and thanks to my supervisor Professor Toshiaki Abe who have been a tremendous mentor for me and have provided encouragement, mentorship, and innumerable, excellent ideas. It has been an honor to be his Ph.D. student. I would also wish to express my deepest gratitude to Dr. Nobuhiro Nagai for his time and countless stimulating discussions, assistance with experiments, numerous advice on the progress of the project and tireless assistance with both experimental and documentary aspects of this project. I would have never been able to accomplish this thesis without his endless and priceless supervision. I am also deeply grateful of Professor Hirokazu Kaji for his outstanding ideas and advice. I am also very thankful to all members of Clinical Cell Therapy laboratory and Biodevice Engineering laboratory since every result described in this thesis was accomplished with the help and support of fellow lab-mates and collaborators.

Finally, I am forever indebted to my family and friends and I would like to express my true love and appreciation to them for their unconditional love, support, and encouragement. They have stood by my side, cherished with me every great moment and supported me at every step.

I would like to dedicate this thesis to my beloved parents whose tremendous love and sacrifice throughout my life made it possible for me to achieve each every single one of my goals.